

# Practical Methods for Solid-State NMR Distance Measurements on Large Biomolecules: Constant-Time Rotational Resonance

Yael S. Balazs and Lynmarie K. Thompson<sup>1</sup>

*Department of Chemistry, University of Massachusetts, Amherst, Massachusetts 01003*

Received January 8, 1999; revised April 20, 1999

**Simple modifications of the rotational resonance experiment substantially reduce the total experimental time needed to measure weak homonuclear dipolar couplings, a critical factor for achieving routine internuclear distance measurements in large biomolecular systems. These modifications also address several problems cited in the literature. Here we introduce a constant-time rotational resonance experiment that eliminates the need for control spectra to correct for effects from variable RF heating, particularly critical for accurate long-distance measurements. This reduces the total number of experiments needed by as much as a factor of 2. Other improvements incorporated include achieving selective inversion with a delay rather than a weak pulse (P. R. Costa *et al.*, *J. Am. Chem. Soc.* **119**, 10487–10493, 1997), which we observe results in the elimination of oscillations in peak intensities for short mixing time points. This reduces the total experiment time in two ways. First, there is no longer a need to average different “zero”-time points (S. O. Smith *et al.*, *Biochemistry* **33**, 6334–6341, 1994) to correct for intensity variations. Second, short-mixing-time lineshape differences observed in large membrane-bound proteins only appear with the weak-pulse inversion and not when using the delay inversion. Consistent lineshapes between short and long mixing times permit the use of a single spectrum for subtraction of natural abundance background signals from all labeled-protein time points. Elimination of these effects improves the accuracy and efficiency of rotational resonance internuclear distance measurements.**

© 1999 Academic Press

**Key Words:** rotational resonance; solid-state NMR; magic-angle spinning; homonuclear dipolar coupling; proteins.

## INTRODUCTION

Solid-state NMR internuclear distance measurements provide a powerful method for directly probing local structure and structural changes in large biomolecules, which can contribute valuable insights into structure and function not possible by any other method. Conventional techniques for structural investigations are limited by the need for rapid tumbling rates for solution NMR, resulting in an upper limit of around 30 kDa, or the need to form high-quality crystals for X-ray diffraction, which is difficult for membrane-bound proteins. Magic-angle

spinning (MAS) solid-state NMR enables high-resolution experiments on immobile or slowly tumbling samples by averaging out  $(3 \cos^2 \theta - 1)$  terms in the chemical shift Hamiltonian, but also averages dipolar couplings, which sacrifices distance information.

Reintroduction of dipolar couplings during magic-angle spinning through rotational resonance (*1*) has already shed light on a variety of biological questions (2–5) [reviewed in (6)]. Rotational resonance, which recouples homonuclear spin pairs, occurs when an integer multiple of the spinning speed equals the difference in isotropic chemical shifts between spins of interest,  $n\nu_r = \Delta\sigma_{\text{iso}}$ . Selective inversion of one resonance creates a difference polarization between the two spins which then undergo rotor-driven magnetization exchange during the mixing time. Through-space internuclear distances are extracted by plotting experimental differences in peak intensity between recoupled spins as a function of mixing time onto simulated exchange curves for different dipolar coupling strengths (*1*). However, internuclear distance measurements between weakly coupled homonuclear spins in systems such as large membrane-bound proteins still present a variety of challenges that must be reliably met before such experiments can be used routinely.

The biggest hurdle when dealing with large biomolecules and weakly coupled systems is the inherently low signal-to-noise. Large biomolecules require specific isotopic labeling to target sites of interest. For instance, observation of a unique site in a 120-kDa homodimeric membrane-bound protein translates into doing experiments on approximately 200 nmol of <sup>13</sup>C spins. To evaluate a few different mixing times, such experiments typically require signal averaging times on the order of days to get intensity differences due to magnetization exchange that are reliably above the noise.

We have developed variations of the standard rotational resonance experiment to eliminate several artifacts previously corrected with additional control spectra. Such improvements are critical for measuring weak couplings where the magnitude of the magnetization exchange can be nearly equal to the corrections. By introducing a constant decoupling time and by using a delay for selective inversion of spin polarization we have significantly improved the reliability of the experiment

<sup>1</sup> To whom correspondence should be addressed. E-mail: [thompson@chem.umass.edu](mailto:thompson@chem.umass.edu). Fax: (413) 545–4490.

and reduced the number of spectra required. Improved reliability and efficiency should increase accessibility of homonuclear distance measurements for a wide variety of biological problems.

## RESULTS AND DISCUSSION

Rotational resonance measurements of long  $^{13}\text{C}/^{13}\text{C}$  internuclear distances (4–6 Å) can suffer from problems that are not immediately apparent when tested on readily available  $^{13}\text{C}_2$  molecules with short internuclear separations. We have chosen such a readily available molecule (1,3- $^{13}\text{C}_2$ -Ala, with a 2.5-Å internuclear separation), typical of those used in most laboratories, to demonstrate that experimental conditions can be chosen to reveal the problems that will occur in a long-distance measurement. First, extending the experiment to the long mixing times needed for long-distance measurements reveals one problem: nonrotational resonance magnetization decay occurs due to probe detuning. This decay is eliminated by the constant-time experiment described below. Second, the rapid magnetization exchange characteristic of short distances can be damped to resemble the slower magnetization decay observed in long-distance measurements by reducing the decoupling field (which decreases  $T_2^{ZQ}$ ). This condition reveals a problem with oscillations in the magnetization at short times (before the start of rotational resonance exchange) which has been previously noted in a membrane peptide system (3, 4). These oscillations are eliminated by using a delay inversion (2) rather than a weak pulse inversion, as described below. Thus these conditions (long mixing times and weak decoupling fields) can be used with readily available  $^{13}\text{C}_2$  molecules as a means of finding and correcting problems specific to long-distance measurements.

### Constant Time

A constant-time version of the rotational resonance experiment was constructed for consistent RF heating during all mixing times, thus reducing the total number of spectra needed by as much as a factor of 2. The constant time is achieved by introducing an additional variable delay before spin inversion. The sum of the “constant-time” delay ( $\tau_d$ ) and the mixing time ( $\tau_{\text{mix}}$ ) is kept the same for all mixing time points to ensure a constant overall high-power decoupling time (Fig. 1). In previous rotational resonance experiments, comparison of spectra collected with and without selective inversion has been used to discriminate loss of intensity due to detuning (caused by RF heating) or due to  $^{13}\text{C}$   $T_1$  decay during the longer mixing times from loss of intensity due to rotor-driven magnetization exchange at the rotational resonance condition (7). For strongly coupled systems a 5–10% correction due to RF heating is tolerable, since it is relatively small compared with the large intensity decrease due to the magnetization exchange. However, in weakly coupled systems where the magnetization

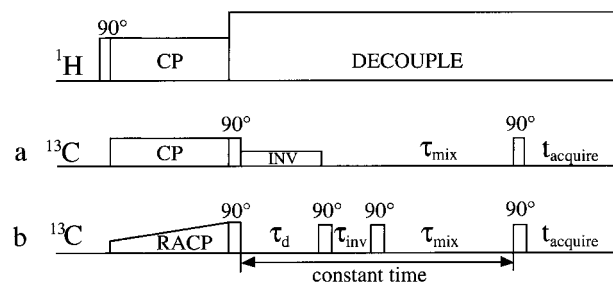


**FIG. 1.** Constant-time rotational resonance pulse sequence. (a) Original rotational resonance pulse sequence ( $J$ ). (b) Constant-time version: The first delay ( $\tau_d$ ), with spins stored along the  $z$  axis, varies in proportion to the mixing time ( $\tau_{\text{mix}}$ ) to conserve a constant time of high-power proton decoupling for all experimental time points. For the inversion delay, the carrier frequency is centered between the two resonances to be recoupled.  $\tau_{\text{inv}}$  is set to  $(2\Delta\sigma_{\text{iso}})^{-1}$  during which the spins of interest precess  $180^\circ$  apart. This delay is immediately followed by a  $90^\circ$  pulse, placing the spins onto  $\pm z$  for the variable mixing time during which rotational resonance magnetization exchange occurs. Cross-polarization (eight-phase cycle) is ramped to maximize efficiency at high spinning speeds (11). The second and final  $^{13}\text{C}$   $\pi/2$  pulses bring the spins onto the  $xy$  plane from each of the four possible directions, resulting in an  $8 \times 4 \times 4 = 128$ -phase cycle.

difference being measured may also be around 10%, corrections are no longer trivial. In addition, since magnetization exchange curves for long distances are simple decays without sinusoidal oscillations, final intensities are critical for defining the curve and obtaining the correct distance. Finally, measurements of long distances require longer mixing times than do shorter distances, resulting in increased RF heating artifacts on these weakly coupled systems.

Figure 2 compares constant-time and nonconstant-time rotational resonance experiments measuring the 2.5-Å distance in 1,3- $^{13}\text{C}_2$ -Ala. Mixing times up to 60 ms with proton decoupling field strengths of  $\gamma B_1/2\pi \sim 70$  kHz were used. Selective inversion creates difference polarization ( $I_1 - I_2 = \Delta_p$ ); its evolution with mixing time yields the dipolar coupling. Identical control spectra without selective inversion are used to determine whether other factors contribute to the magnetization decay, by plotting the sum polarization ( $I_1 + I_2 = \Sigma_p$ ) versus mixing time. Using a constant decoupling time prevents nonrotational resonance intensity losses in the control spectra and the sum magnetization ( $\Sigma_p$ ) remains constant for all mixing times. Without using constant-time rotational resonance, the sum magnetization decreases to 0.63 at 60 ms, an intensity decrease comparable to the calculated rotational resonance exchange curve for a  $\sim 5$ -Å distance (with  $T_2^{ZQ} = 2$  ms and chemical shift dispersion). Thus, with the nonconstant-time experiment the decay due to RF heating or  $^{13}\text{C}$   $T_1$  can be the same as or larger than the decay from magnetization exchange in a weakly coupled spin pair. The magnitude of the decay due to RF heating is likely to vary for different probes and decoupling powers. The magnitude of the decay due to  $^{13}\text{C}$   $T_1$  will be small at these mixing times (shortest  $T_1$  values expected are  $\sim 600$  ms for  $\text{CH}_3$  groups, predicting 10%  $T_1$  decay at 60 ms).

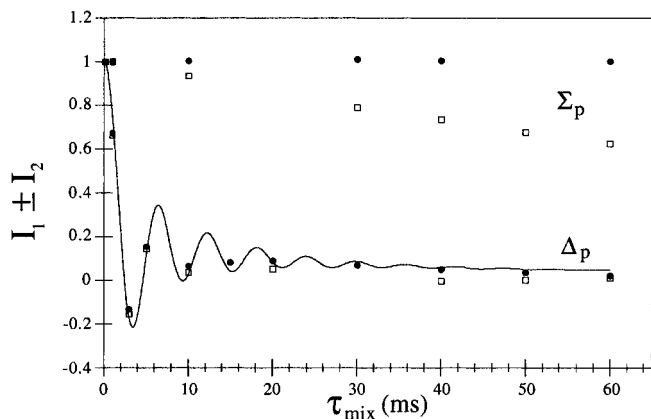


**FIG. 2.** Constant-time (●) versus nonconstant-time (□) rotational resonance on 1,3- $^{13}\text{C}_2$ -Ala.  $\Sigma_p$  indicates sum polarization—the sum of the peak areas for the carboxyl and methyl groups without a selective inversion. Without constant-time rotational resonance this value decreases due to detuning under RF heating which reduces signal intensity.  $\Delta_p$  indicates difference polarization—the difference between the peak areas for the carboxyl and methyl groups with selective inversion of the methyl peak. The solid line is the simulated  $n = 1$  rotational resonance curve for an internuclear distance of 2.5 Å, with the following parameters:  $T_2^{ZQ} = 9$  ms (estimated as  $1/T_2^{ZQ} = 1/T_2(\text{CH}_3) + 1/T_2(\text{COOH})$ , with  $T_2$  values measured with CP- $\tau$ -180- $\tau$ -AQ); chemical shift tensor values [from (12)] of  $\delta = 5.283$  kHz,  $\eta = 0.84$  (carboxyl),  $\delta = 0.906$  kHz,  $\eta = 0.75$  (methyl); and Euler angles relating the shift tensor to the dipolar tensor of (0, 58, 0) carboxyl and (0, 33, 0) methyl, deduced from the crystal structure of alanine (13). The  $\Delta_p$  data are plotted without correction for the  $\Sigma_p$  decays. Both experiments give an internuclear distance of 2.5 Å in agreement with previous measurements (5, 13).

Note that this problem would not be apparent in a rotational resonance experiment on a short-distance standard such as alanine because of the very rapid decay of the difference magnetization. Corrections to the difference magnetization for the decay of the control spectra without inversion are insignificant and are not needed to obtain the correct 2.5-Å distance (Fig. 2).

It should be noted that even the constant-time version of the experiment does not correct perfectly for  $^{13}\text{C}$   $T_1$  decay, because the state of the system differs between the  $\tau_d$  period (both spins on  $+z$ ) and the  $\tau_{\text{mix}}$  period (spins on  $\pm z$ ). There is no differential  $T_1$  effect with mixing time for the spin that is on  $+z$  during both periods. However, the spin that is inverted will experience different  $T_1$  decay with different mixing times. Thus any experiment involving a spin with a short  $T_1$  (e.g., methyl carbon) should be performed with inversion at the other (long  $T_1$ ,  $> \text{s}$ ) site. Then differential  $T_1$  decay is unlikely to cause any nonrotational resonance decays in the constant-time experiment.

The phase cycling scheme chosen for the constant-time rotational resonance pulse sequence succeeds in canceling out all residual magnetization in the  $xy$  plane arising from imperfect and/or misset  $\pi/2$  pulses and missettings of the inversion delay. This was demonstrated on unlabeled glycine by deliberately missetting the  $\pi/2$  pulses or the inversion delay by as

much as 50% and observing no change in intensities between long and short mixing times. Since in natural abundance glycine there is only a 0.01% occurrence of  $^{13}\text{C}$ -carboxyl directly bonded to  $^{13}\text{C}\alpha$ , there should not be any detectable change in peak intensities due to rotational resonance magnetization exchange. Without the full 128-phase cycle, decay between short and long mixing times is apparent due to  $T_2$  decay of residual magnetization in the  $xy$  plane (data not shown). In the case of large biomolecules, where a large number of scans are inherently required, there is no disadvantage to having a long phase-cycling scheme.

Another reduction in the number of control spectra needed is achieved by cycling between all time points. If data are collected for different mixing times sequentially, it is often necessary to collect additional spectra (e.g., repeat the zero-mixing-time spectrum) to check for instrumental drift over the long experiment times ( $\sim \text{days}$ ). It is more efficient to collect data in blocks of 128 transients per mixing time and cycle through the series of mixing times to be sampled (“multicyc” command in Bruker software). Thus any instrumental drifts are equally experienced by each mixing time.

Constant-time rotational resonance has additional advantages for long-distance measurements in cases where a unique resolved spin is undergoing exchange with a small fraction of multiple, unresolved spins. Such a scenario is typical in large biomolecules produced biosynthetically, since single labels are often limited to unique amino acids, ligands, or cofactors. In particular, constant-time rotational resonance is preferable where the sum of intensity losses due to RF heating or  $^{13}\text{C}$   $T_1$  decay at the abundant nonexchanging sites would otherwise exceed the small intensity decrease due to magnetization exchange at the single spin pair of interest. Another advantage is the opportunity to do a single-site analysis, focusing on the unique site. Since the sum of the peaks in the inverted spectrum remains constant throughout magnetization exchange ( $I_1 + I_2 = C$ ), it is possible to evaluate the rotational resonance of the difference polarization in terms of one of the resonances ( $I_1 - I_2 = C - 2I_2$ ). For the 1,3- $^{13}\text{C}_2$ -Ala sample shown in Fig. 2, the standard deviation for  $I_1 + I_2 = C$  in the inverted spectrum is 15% through 50 ms of exchange with the constant-time experiment, compared with a 30% standard deviation for the nonconstant-time pulse sequence. Thus, the constant time experiment improves the validity of a single-site analysis.

### Delay Inversion

We observe that achieving selective inversion via a delay (2, 7) [ $\pi/2 - \tau_{\text{inv}} - \pi/2$ , where  $\tau_{\text{inv}} = (2\Delta\sigma_{\text{iso}})^{-1}$  with the carrier frequency centered between the two resonances] offers several advantages over creating  $\pm z$  polarization through a weak inversion pulse with the carrier frequency centered on the peak to be inverted. The weak pulse inversion takes  $\sim 400 \mu\text{s}$ , a long period during which ambiguous effects may occur. In contrast the delay inversion occurs at the second hard  $\pi/2$  pulse ( $\sim 4$

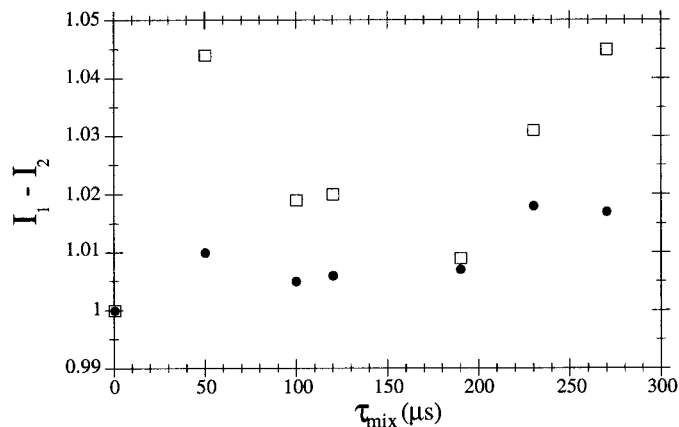


**FIG. 3.** Selective inversion methods differ in zero-time-point reliability. Data for 1,3- $^{13}\text{C}_2$ -Ala with low power proton decoupling fields ( $\gamma B_1/2\pi < 40$  kHz) during the rotational resonance mixing time. Under these conditions magnetization exchange due to rotational resonance is not observed until  $\tau_{\text{mix}} = 500 \mu\text{s}$ . Weak-pulse selective inversions ( $\square$ ) display peak intensity variations at short mixing times, as cited in the literature (3, 4). However, time-delay inversions ( $\bullet$ ), taking two orders of magnitude less time to invert spins, do not undergo short mixing time fluctuations. Thus, a single spectrum gives a reliable “zero-mixing-time” point.

$\mu\text{s}$ ). Because the delay is quite short ( $\tau_{\text{inv}} = 40\text{--}50 \mu\text{s}$ ), there is no significant rotational resonance exchange or  $T_2$  relaxation (even for the shortest  $\text{CH}_2$   $T_2$ 's  $\sim 1$  ms).

One problematic effect that occurs with the weak pulse, but not with the delay method is a fluctuation in peak intensity during short mixing times before rotational resonance magnetization exchange begins (Fig. 3). For strongly coupled systems the subtle oscillations are masked by rapid decays in intensities due to magnetization exchange. Therefore we used low proton decoupling fields ( $\gamma B_1/2\pi < 40$  kHz) to decrease  $T_2^{ZQ}$  and damp the rapid rotational resonance oscillations on the 1,3- $^{13}\text{C}_2$ -Ala sample. These conditions reveal intensity fluctuations occurring before the start of rotational resonance exchange, when a weak pulse inversion is used (Fig. 3, open squares). Under the same conditions, the delay inversion method (Fig. 3, filled circles) reduces the intensity fluctuations. Measuring an accurate zero mixing time is essential for getting a correct internuclear distance measurement because subsequent mixing times are normalized to this initial time point. A consistent value for short mixing times increases the reliability of the final distance determination and eliminates the need to average three or four intensities for mixing times less than 1 ms (3, 4). This saves considerably on the overall number of spectra needed to accurately measure an internuclear distance.

The delay inversion method also yields consistent phasing and lineshapes for the series of spectra. For the short mixing times under 300  $\mu\text{s}$  shown in Fig. 3, using the delay inversion results in correct phasing for all spectra using identical phasing parameters. However, the weak-pulse inversion spectra would not properly phase with a single set of phasing parameters (data

not shown). For the natural abundance spectrum of a large, membrane-bound protein (120-kDa homodimer bound to bacterial inner-membrane vesicles) we observed a difference in lineshape between the short and long mixing times when using a weak pulse inversion. For the delay inversion, both short and long time points had the same lineshape (Fig. 4). The practical result of consistent lineshapes is that a single unlabeled protein spectrum can then be used for all subtractions of 1% natural abundance  $^{13}\text{C}$  background signals. This reduces the total number of spectra required and increases confidence in the normalized experimental data used to determine internuclear distances.

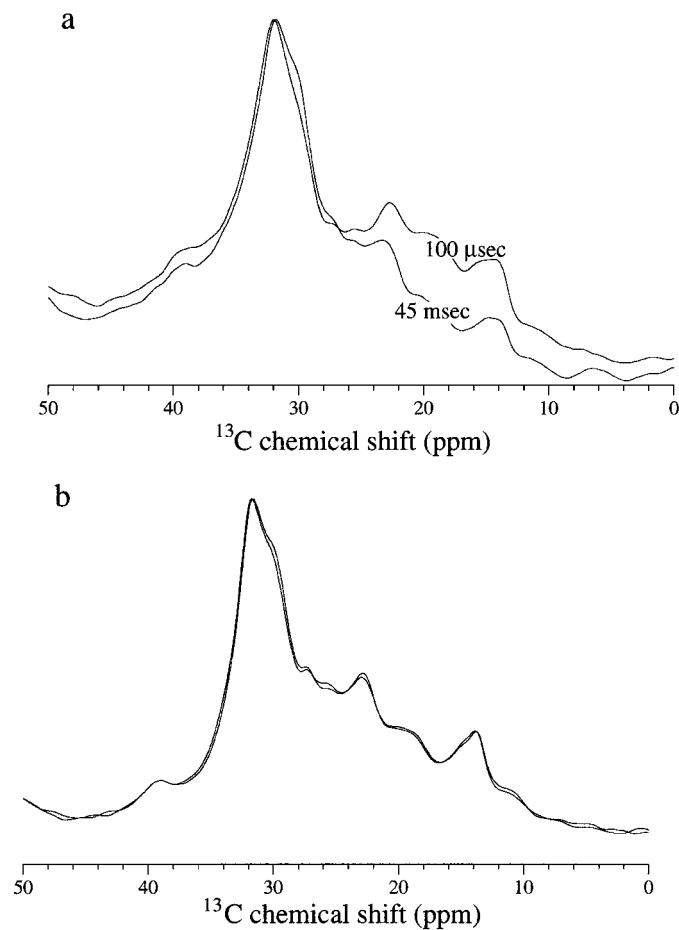


**FIG. 4.** Effects of weak pulse versus delay inversions on lineshapes.  $^{13}\text{C}$  spectra, noninverted region, of  $\sim 216$  nmol unlabeled transmembrane bacterial chemotaxis receptors bound to native inner-membrane vesicles, 32,000 scans each without constant decoupling times,  $-5^\circ\text{C}$ . Each pair of spectra have the same phasing parameters. No rotational resonance should be observed on this sample. (a) The selective weak-pulse inversion shows a different pattern of peak intensities for short (100  $\mu\text{s}$ ) versus long (45 ms) mixing times. (b) With the time-delay inversion the 100- $\mu\text{s}$  mixing time spectrum is indistinguishable from the 45-ms mixing time spectrum. Thus with a delay-inversion one unlabeled spectrum can be used for all natural abundance subtractions for improved reliability and efficiency.

## CONCLUSIONS

The constant-time rotational resonance experiment for measuring homonuclear distances shows no decay in intensities due to variable RF heating commensurate with mixing times. We have also demonstrated that using a delay inversion results in reliable peak intensities at short mixing times and consistent phasing and lineshapes for all mixing times. These easy-to-employ modifications to rotational resonance eliminate the need for multiple control spectra, increasing the reliability of the measurement and significantly reducing the experiment time. This provides an efficient approach for performing accurate rotational resonance internuclear distance measurements on large biomolecules.

## EXPERIMENTAL

As a standard for dipolar coupling measurements, DL-alanine-1,3-<sup>13</sup>C<sub>2</sub>-<sup>15</sup>N (<sup>13</sup>C, 99%; <sup>15</sup>N, 99%) was obtained from Cambridge Isotope Labs (Andover, MA) and diluted ninefold with unlabeled alanine to avoid intermolecular dipolar interactions, dissolved in H<sub>2</sub>O, and lyophilized. Unlabeled bacterial inner-membrane vesicles containing membrane-bound bacterial chemotaxis receptors were isolated from an auxotrophic *Escherichia coli* strain containing the overexpression vector pHSe5.tsr, according to protocols described elsewhere (8, 9). Wet membrane-protein pellets were collected at 45,000 rpm (Beckman Ultracentrifuge Ti70 rotor) for 2 h at 4°C and stored at -70°C until packed into a 4-mm zirconia rotor.

<sup>13</sup>C solid-state NMR experiments were performed on a Bruker ASX300 spectrometer. The samples were packed in 4-mm zirconia Bruker rotors fitted with Kel-F end caps for magic-angle spinning at ≤15 kHz. The magic-angle spinning speed controller keeps spinning rate fluctuations to less than ±3 Hz. Spectrometer tuning frequencies were 300.13 MHz for <sup>1</sup>H and 75.47 MHz for <sup>13</sup>C. Ramped cross-polarization (1.5-ms contact times and an 18% ramp on the X channel) was performed with proton decoupling field strengths of  $\gamma B_1/2\pi \sim 50$  kHz. The power was increased to provide ~69-kHz <sup>1</sup>H decoupling fields during rotational resonance magnetization exchange and acquisition times. Rotational resonance experiments on 1,2-<sup>13</sup>C<sub>2</sub>-Ala were performed with magic-angle spinning at 11,862 Hz ( $n = 1$ ) and 5- $\mu$ s <sup>1</sup>H and <sup>13</sup>C 90° pulse lengths. Weak pulse inversions used a 400- $\mu$ s inversion pulse (carrier frequency on resonance to be inverted). Delay inversions used  $\tau_{\text{inv}} = 1/2\Delta\sigma_{\text{iso}}$  (carrier frequency centered between the two resonances). <sup>13</sup>C chemical shifts were referenced to the methyl peak of 1,4-di-*tert*-butylbenzene at 31 ppm.

Sample temperatures were calibrated by an external standard of tetrakis(trimethylsilyl)silane (98%; Sigma-Aldrich, St. Louis, MO) soaked in liquid methanol and packed into a 4-mm rotor under a nitrogen environment. The temperature standard was spun under identical MAS speeds and thermocouple readout temperatures as experimental samples to obtain the actual temperatures of

the material in the rotor after frictional heating by high MAS speeds. The difference in the <sup>1</sup>H chemical shift of the methyl and hydroxyl peaks was fit to the modified equation of van Geet given by Aliev and Harris (10) scaled to 300 MHz to determine the calibrated sample temperature. Spectra on the labeled alanine were collected at a calibrated temperature of 35°C with a 1.5-s recycle delay. For spectra of frozen membrane protein samples, extended periods of signal averaging with sample cooling were achieved by using dry air (dried with a Balston Instrument air dryer) for the spinning and cooling gases; the latter was cooled in a bath of Cryocool fluid (Savant Instruments, Inc., Farmingdale, NY) containing a CC-100II immersion cooler (NESLAB Instruments, Inc., Portsmouth, NH), followed by a second cold bath of Cryocool fluid cooled with dry ice pellets. The second Cryocool bath was critical to provide sufficient cooling of the protein sample to compensate for frictional heating at high spinning speeds. All four spectra of frozen membrane protein (Fig. 4) were collected in one experiment, cycling between blocks of 32 transients each (total of 32,000 scans each) without constant-time decoupling and at a calibrated temperature of -5°C with a 1-s recycle delay.

Natural abundance corrections for unlabeled alanine contributions not undergoing rotational resonance magnetization exchange were made on the integrated area differences before normalization. Unlabeled alanine with 1% <sup>13</sup>C is present in ninefold excess, contributing 0.09 to the total peak, whereas the 1 part DL-alanine-1,3-<sup>13</sup>C<sub>2</sub>-<sup>15</sup>N is 99% labeled. Thus, the correction is made by subtracting 0.09/(0.09 + 0.99) of the zero-time point integrated area difference from each of the time points before normalization. Error bars corresponding to ± one standard deviation of the spectral noise were smaller than the symbol sizes used in the plots.

## ACKNOWLEDGMENTS

This research was supported by U.S. Public Health Service Grant GM47601, an award from Research Corporation, and a NSF Young Investigator Award (to L.K.T.). Y.S.B. was supported in part by National Research Service Award T32 GM08515 from the National Institutes of Health.

The NMR instrument was purchased with a grant from the NSF (BIR-911996) and funds from the University of Massachusetts, and is partially supported by the NSF Materials Research Science and Engineering Center at the University.

The authors thank Phil Costa, Malcom Levitt, and Robert Griffin for cc2z (M.L.) and rsq2spin (P.C.) programs for simulations of rotational resonance magnetization exchange and for helpful discussions. We also thank Malcom Levitt for suggesting use of a delay inversion and Charlie Dickinson for instrumentation support and helpful discussions.

## REFERENCES

1. D. P. Raleigh, M. H. Levitt, and R. G. Griffin, Rotational resonance in solid-state NMR, *Chem. Phys. Lett.* **146**, 71-76 (1988).
2. P. R. Costa, D. A. Kocisko, B. Q. Sun, P. T. Lansbury, Jr., and R. G. Griffin, Determination of peptide amide configuration in a model amyloid fibril by solid-state NMR, *J. Am. Chem. Soc.* **119**, 10487-10493 (1997).

3. S. O. Smith, R. Jonas, M. Braiman, and B. J. Bormann, Structure and orientation of the transmembrane domain of glycoprotein A in lipid bilayers, *Biochemistry* **33**, 6334–6341 (1994).
4. S. O. Smith, J. Hamilton, A. Salmon, and B. J. Bormann, Rotational resonance NMR determination of intra- and intermolecular distance constraints in dipalmitoylphosphatidylcholine bilayers, *Biochemistry* **33**, 6327–6333 (1994).
5. J. M. Griffiths, T. T. Ashburn, M. Auger, P. R. Costa, R. G. Griffin, and P. T. Lansbury, Jr., Rotational resonance solid-state NMR elucidates a structural model of pancreatic amyloid, *J. Am. Chem. Soc.* **117**, 3539–3546 (1995).
6. J. R. Garbow and T. Gullion, Measurement of internuclear distances in biological solids by magic-angle spinning  $^{13}\text{C}$  NMR, in "Carbon-13 NMR Spectroscopy of Biological Systems" (N. Beckman, Ed.), pp. 65–115, Academic Press, San Diego (1995).
7. P. R. Costa, B. Sun, and R. G. Griffin, Rotational resonance tickling: Accurate internuclear distance measurement in solids, *J. Am. Chem. Soc.* **119**, 10821–10830 (1997).
8. J. A. Gegner, D. R. Graham, A. F. Roth, and F. W. Dahlquist, Assembly of an MCP receptor, CheW, and kinase CheA complex in the bacterial chemotaxis signal transduction pathway, *Cell* **70**, 975–982 (1992).
9. J. Wang, Y. S. Balazs, and L. K. Thompson, Solid-state REDOR distance measurements at the ligand site of a bacterial chemotaxis receptor, *Biochemistry* **36**, 1699–1703 (1997).
10. A. E. Aliev and K. D. M. Harris, Simple technique for temperature calibration of a MAS probe for solid-state NMR spectroscopy, *Magn. Reson. Chem.* **32**, 366–369 (1994).
11. G. Metz, X. Wu, and S. O. Smith, Ramped-amplitude cross polarization in magic-angle-spinning NMR, *J. Magn. Reson. A* **110**, 219–227 (1994).
12. W. S. Veeman, Carbon-13 chemical shift anisotropy, *Prog. NMR Spectrosc.* **16**, 193–235 (1984).
13. J. Donohue, The crystal structure of DL-alanine. II. Revision of parameters by three-dimensional Fourier analysis, *J. Am. Chem. Soc.* **72**, 949–953 (1950).